Published for SISSA by Springer

Received: *April 22, 2017*
Accepted: *June 8, 2017*
Published: *June 14, 2017*

Holographic micro thermofield geometries of BTZ black holes

Dongsu Bak,[a,e] **Chanju Kim,**[b] **Kyung Kiu Kim**[c] **and Jeong-Pil Song**[d]

[a] *Physics Department, University of Seoul, Seoul 02504, Korea*
[b] *Department of Physics, Ewha Womans University, Seoul 03760, Korea*
[c] *Department of Physics, Sejong University, Seoul 05006, Korea*
[d] *Department of Chemistry, Brown University, Providence, Rhode Island 02912, U.S.A.*
[e] *Center for Theoretical Physics of the Universe, Institute for Basic Science, Seoul 08826, Korea*

E-mail: dsbak@uos.ac.kr, cjkim@ewha.ac.kr, kimkyungkiu@sejong.ac.kr, jeong_pil_song@brown.edu

Abstract: We find general deformations of BTZ spacetime and identify the corresponding thermofield initial states of the dual CFT. We deform the geometry by introducing bulk fields dual to primary operators and find the back-reacted gravity solutions to the quadratic order of the deformation parameter. The dual thermofield initial states can be deformed by inserting arbitrary linear combination of operators at the mid-point of the Euclidean time evolution that appears in the construction of the thermofield initial states. The deformed geometries are dual to thermofield states without deforming the boundary Hamiltonians in the CFT side. We explicitly demonstrate that the AdS/CFT correspondence is not a linear correspondence in the sense that the linear structure of Hilbert space of the underlying CFT is realized nonlinearly in the gravity side. We also find that their Penrose diagrams are no longer a square but elongated horizontally due to deformation. These geometries describe a relaxation of generic initial perturbation of thermal system while fixing the total energy of the system. The coarse-grained entropy grows and the relaxation time scale is of order $\beta/2\pi$. We clarify that the gravity description involves coarse-graining inevitably missing some information of nonperturbative degrees.

Keywords: AdS-CFT Correspondence, Black Holes, Conformal Field Theory

ArXiv ePrint: 1704.01030

doi:10.1007/JHEP06(2017)079

JHEP06(2017)079

Contents

1 Introduction

Currently there are many available examples of AdS/CFT correspondence [1–3], from which one may study various aspects of gravity and field theories in a rather precisely defined setup. Numerous aspects of strongly coupled field theories have been understood by studying the bulk dynamics based on the AdS/CFT correspondence. However understanding certain aspects of gravity system are still lacking, which in particular include degrees behind horizon and gravitational singularities.

In this note, we focus on the gravity dynamics based on the 3d BTZ black hole [4]/ thermofield double [5] correspondence which was first introduced in [6]. Here we consider three dimensional case only, which of course can be generalized to other dimensions. An interesting deformation [7, 8] of thermofield double system has appeared based on the Janus geometries [7, 9]. The deformation makes the systems living in the left and the right boundaries of the BTZ black hole different from each other with an exactly marginal operator turned on. The corresponding black hole solution becomes time-dependent, which is called as Janus time-dependent black hole (TDBH). The corresponding thermofield initial state of the boundary CFT involves an Euclidean time evolution $U = e^{-\frac{\beta}{4}H_R}e^{-\frac{\beta}{4}H_L}$ where $H_{L/R}$ is respectively for the Hamiltonian of the left/right system and β is the inverse of

JHEP06(2017)079

the late-time equilibrium temperature. Looking at the system from the viewpoint of one boundary, the Janus TDBH solution describes thermalization of an initial perturbation of thermal system. Namely the above deformation brings the system an initially out-of-equilibrium state, which will be exponentially relaxed away by thermalization leading to the equilibrium state. This late time behaviors are basically controlled by the physics of quasi-normal modes. Thus the late-time regime is in a quasi-equilibrium but, in general, the system is not even in a quasi-equilibrium under relaxation, during which the thermodynamic variables such as temperature and free energy are not well defined.

In this note, we shall consider rather generic perturbations of the BTZ geometry in the framework of the AdS/CFT correspondence, for which the boundary Hamiltonians remain intact. The thermofield initial states of the system, however, can still be deformed rather generically, which is followed by a time evolution by undeformed Hamiltonians. This will be achieved by inserting an arbitrary linear combination of operators at the mid-point of the Euclidean time evolution as $U = e^{-\frac{\beta}{4}H_0} e^{-\sum_I C_I O_I} e^{-\frac{\beta}{4}H_0}$ with H_0 denoting the undeformed BTZ Hamiltonian. Based on the operator-state correspondence, a rather generic perturbation of thermal system can be achieved. Namely such states are still particularly entangled from the viewpoint of a two sided observer. These out-of-equilibrium perturbations will be exponentially relaxed away in the far future. Thus the deformations are describing thermalization of generic perturbation of thermal system. We illustrate these using scalar primary operators dual to bulk scalar fields. Below we shall find the explicit solution of the scalar field to the leading order which takes a rather simple form. We solve the back-reacted geometries to the quadratic order of the scalar perturbation parameter which we take as γ.

These geometries have many interesting applications. These may be viewed as a realization of micro thermofield deformations of the BTZ geometry. We argue that the bulk observer of a particular side cannot extract the full microscopic information available in the reduced density matrix of the same side by studying the perturbative gravity dynamics including full back-reactions. The micro-geometries are also expected to play an important role in understanding the behind-horizon degrees, which is beyond the scope of the present work.

In section 2, we present the three dimensional AdS Einstein scalar system and the BTZ background. In section 3, we present the perturbation equations including the gravity back-reactions to their leading order. We solve these gravity equations for the simplest perturbation of the $m^2 = 0$ scalar field. We analyze the deformation of the corresponding Penrose diagram and horizon area. In section 4, we present the field theory description of the above perturbation. In section 5, we generalize the above construction to micro-geometries corresponding to other deformations of thermofield states. In section 6, we describe the bulk dynamics and their decoding problem. Last section is devoted to our concluding remarks. In appendices, we present more examples of gravity solutions for various scalar perturbations.

Note added: upon preparing the submission, there appeared a paper [19], whose results partially overlap with ours in this paper.

JHEP06(2017)079

2 Einstein scalar system

We begin with the three dimensional Einstein scalar system

$$S = \frac{1}{16\pi G}\int d^3x\sqrt{-g}\left(R + \frac{2}{\ell^2} - g^{ab}\partial_a\phi\partial_b\phi - m^2\phi^2\right) \tag{2.1}$$

One may turn on linear combination of the above bulk scalar fields or even other bulk fields with non-zero spins. Here we shall limit our consideration to the case of scalar fields. There are also in general interactions between these bulk fields, which we shall ignore in this note. The dimension Δ of the corresponding dual operator is related to the mass by

$$\Delta(\Delta - d) = \ell^2 m^2 \tag{2.2}$$

where d is the spacetime dimension of the boundary CFT which equals 2 for the present case. For the $m^2 = 0$ case, this theory can be fully consistently embedded into type IIB gravity [7]. For non-zero m^2 that corresponds to integral dimensions, the solution can be consistently embedded into IIB supergravity only for the leading order fluctuations including the gravity back reaction. Here we set the AdS radius ℓ to be unity for simplicity and recover it whenever it is necessary. The Einstein equation reads

$$R_{ab} + \left(\frac{2}{\ell^2} - m^2\phi^2\right) g_{ab} = \partial_a\phi\partial_b\phi \tag{2.3}$$

and the scalar equation of motion is given by

$$\nabla^2\phi - m^2\phi = 0 \tag{2.4}$$

Any resulting solutions involving nontrivial scalar field will be deformations of the well known $\mathrm{AdS}_3 \times S^3 \times M_4$ background where M_4 may be either T^4 or $K3$ [10]. Thus our construction is based on this full microscopic AdS/CFT correspondence.

The BTZ black hole in three dimensions can be written as

$$ds^2 = -\frac{r^2 - R^2}{\ell^2}dt^2 + \frac{\ell^2}{r^2 - R^2}dr^2 + r^2 d\varphi^2 \tag{2.5}$$

where the coordinate φ is circle compactified with $\varphi \sim \varphi + 2\pi$. Of course here we turn off the scalar field. Note that the horizon is located at $r = R$. The regularity near $r = R$ is ensured if the Euclidean time coordinate t_E has a period $\beta = 2\pi\frac{\ell^2}{R}$. The corresponding Gibbons-Hawking temperature is then

$$T = \frac{R}{2\pi\ell^2} \tag{2.6}$$

The mass of the black hole can be identified as

$$M = \frac{R^2}{8G\ell^2} \tag{2.7}$$

The boundary system is defined on a cylinder

$$ds_B^2 = -dt^2 + \ell^2 d\varphi^2 \tag{2.8}$$

JHEP06(2017)079

whose spatial size is given by $L = 2\pi\ell$. The central charge of the boundary conformal field theory is related to the Newton constant by

$$c = \frac{3\ell}{2G} \tag{2.9}$$

Thus the entropy of the system becomes

$$S = \frac{2\pi R}{4G} = \frac{c\pi}{3} T\, 2\pi\ell \tag{2.10}$$

while the energy of the system can be expressed as

$$M = \frac{c\pi}{6} T^2\, 2\pi\ell \tag{2.11}$$

in terms of the quantities of CFT.

3 Linearized perturbation

Introducing new coordinates (τ, μ, x) defined by

$$\begin{aligned} \frac{r}{R} &= \frac{\cos\tau}{\cos\mu} \\ \tanh\frac{tR}{\ell^2} &= \frac{\sin\tau}{\sin\mu} \\ x &= \frac{R}{\ell}\varphi \end{aligned} \tag{3.1}$$

the BTZ black hole metric (2.5) can be rewritten as

$$ds^2 = \frac{\ell^2}{\cos^2\mu}\left[-d\tau^2 + d\mu^2 + \cos^2\tau dx^2\right] \tag{3.2}$$

Motivated by the form of the above metric, we shall make the following ansatz

$$\frac{ds^2}{\ell^2} = \frac{-d\tau^2 + d\mu^2}{A(\tau,\mu,x)} + \frac{dx^2}{B(\tau,\mu,x)}, \qquad \phi = \phi(\tau,\mu,x) \tag{3.3}$$

which describes general static geometries. It is then straightforward to show that the equations of motion (2.3) and (2.4) reduce to

$$\begin{aligned} &(\vec{\partial}A)^2 + \frac{B}{2A}(\partial_x A)^2 - A\,\vec{\partial}^2 A = 2A - \ell^2 m^2 A\phi^2 - A^2\,(\vec{\partial}\phi)^2 + AB\,(\partial_x\phi)^2 \\ &3(\vec{\partial}B)^2 - 2B\,\vec{\partial}^2 B + \frac{6B^3}{A^3}(\partial_x A)^2 - \frac{2B^2}{A^2}\left(\partial_x A\partial_x B + 2B\partial_x^2 A\right) \\ &\qquad\qquad = \frac{B^2}{A}(8 - 4\ell^2 m^2\phi^2 - 4B(\partial_x\phi)^2) \\ &\vec{\partial}B\cdot\vec{\partial}\phi + 2\frac{B^2}{A^2}\partial_x A\partial_x\phi - \frac{B}{A}\partial_x B\partial_x\phi - 2B\,\vec{\partial}^2\phi - 2\frac{B^2}{A}\partial_x^2\phi + 2\ell^2 m^2\frac{B}{A}\phi = 0, \end{aligned} \tag{3.4}$$

where we introduced the notation $\vec{\partial} = (\partial_\tau, \partial_\mu)$ with inner product with metric $\eta_{ij} = \mathrm{diag}(-1, +1)$. This solves the full equations of motion up to some extra integration constants. Using the remaining components of equations of motion, these integration constant should be fixed further.

JHEP06(2017)079

As a power series in γ, the scalar field may be expanded as

$$\phi(\tau,\mu,\varphi)=\sum_{n=0}^{\infty}\gamma^{2n+1}\phi_{(2n+1)}(\tau,\mu,\varphi) \tag{3.5}$$

where we resume the general dependence on the coordinate φ. Then the scalar equation in the leading order becomes

$$\tan\mu\,\partial_\mu h+\tan\tau\,\partial_\tau h+\vec{\partial}^2 h-\frac{\ell^2m^2}{\cos^2\mu}\,h+\frac{\ell^2}{R^2\cos^2\tau}\partial_\varphi^2\,h=0 \tag{3.6}$$

where $h(\tau,\mu,\varphi)$ denotes $\phi_{(1)}(\tau,\mu,\varphi)$. By separation of variables, one may try the ansatz $h(\tau,\mu)\cos j\varphi$ and $h(\tau,\mu)\sin j\varphi$ with $j=0,1,2,\cdots$. Here for simplicity, we shall consider only the case $j=0$ in which the above equation becomes

$$\tan\mu\,\partial_\mu h+\tan\tau\,\partial_\tau h+\vec{\partial}^2 h-\frac{\ell^2m^2}{\cos^2\mu}\,h=0 \tag{3.7}$$

In the following, we will construct the most general solutions of this equation for the mass corresponding to integral dimensions.

The leading perturbation of the metric part begins at $O(\gamma^2)$ with even powers of γ only. Let us organize the series expansions of the metric variables by

$$A=A_0\left(1+\frac{\gamma^2}{4}a(\tau,\mu)+O(\gamma^4)\right),\quad B=B_0\left(1+\frac{\gamma^2}{4}b(\tau,\mu)+O(\gamma^4)\right), \tag{3.8}$$

where

$$A_0=\cos^2\mu,\quad B_0=\frac{\cos^2\mu}{\cos^2\tau} \tag{3.9}$$

The leading order equations for the metric part then become

$$-2a+\cos^2\mu\,\vec{\partial}^2 a\;=\;+4\cos^2\mu(\vec{\partial}h)^2+4\ell^2m^2\,h^2, \tag{3.10}$$

$$\sin 2\mu\,\partial_\mu b+2\cos^2\mu\tan\tau\,\partial_\tau b+\cos^2\mu\,\vec{\partial}^2 b\;=\;+4a+8\ell^2m^2h^2 \tag{3.11}$$

These linear partial differential equations (with the source term), (3.7), (3.10) and (3.11) are of our main interest below. As we discussed before, this set solves the full equations of motion up to some extra homogeneous solutions. Using the remaining components of equations of motion, these coefficients of extra homogeneous solutions should be fixed further. In this section, we shall be working in the case of $m^2=0$ for which one has $\Delta=2$ with the simplest solution of (3.7).

3.1 Linearized solution including back reaction

We begin with a following solution of the leading order scalar equation

$$h=\cos^2\mu\sin\tau \tag{3.12}$$

The solution of (3.10) and (3.11) for the geometry part can be organized as

$$\begin{aligned}a\;&=\;\alpha_0(\mu)+\alpha_1(\mu)\cos 2\tau\\ b\;&=\;\beta_0(\mu)+\beta_1(\mu)\cos 2\tau\end{aligned} \tag{3.13}$$

JHEP06(2017)079

where

$$\begin{aligned}
\alpha_0 &= \frac{1}{64}(1+6\cos 2\mu+5\cos 4\mu)+c_1\tan\mu+\frac{21}{16}(1+\mu\tan\mu)\\
\alpha_1 &= -\frac{1}{16}(5+\cos 4\mu+6\mu(2+\cos 2\mu)\tan\mu)+c_3\cos^2\mu+c_4(2+\cos 2\mu)\tan\mu\\
\beta_0 &= c_2-\frac{1}{16}(13+16c_3)\cos^2\mu+\frac{3}{8}\cos^4\mu+\left(-2c_4+\frac{3}{4}\mu\right)\cos\mu\sin\mu\\
&\quad+\left(c_1+\frac{21}{16}\mu\right)\tan\mu)\\
\beta_1 &= -\frac{1}{32}+\frac{c_3}{2}-\frac{5}{16}\cos 2\mu-\frac{3}{32}\cos 4\mu+\left(c_4-\frac{3}{8}\mu\right)\tan\mu
\end{aligned}\tag{3.14}$$

We then set all the odd homogeneous terms to zero by requiring $c_1 = c_4 = 0$. Then

$$\begin{aligned}
\alpha_0 &= \frac{1}{64}(1+6\cos 2\mu+5\cos 4\mu)+\frac{21}{16}(1+\mu\tan\mu)\\
\alpha_1 &= -\frac{1}{16}(5+\cos 4\mu+6\mu(2+\cos 2\mu)\tan\mu)+c_3\cos^2\mu\\
\beta_0 &= c_2-\frac{1}{16}(13+16c_3)\cos^2\mu+\frac{3}{8}\cos^4\mu+\frac{3}{4}\mu\cos\mu\sin\mu+\frac{21}{16}\mu\tan\mu\\
\beta_1 &= -\frac{1}{32}+\frac{c_3}{2}-\frac{5}{16}\cos 2\mu-\frac{3}{32}\cos 4\mu-\frac{3}{8}\mu\tan\mu
\end{aligned}\tag{3.15}$$

To fix the remaining coefficients c_2 and c_3, now note that the metric functions A and B in (3.8) can be written in more convenient forms

$$\begin{aligned}
\cos^2\mu\left(1+\frac{\gamma^2}{4}(\alpha_0+\alpha_1\cos 2\tau)\right) &= \frac{\cos^2\kappa\mu}{\kappa^2}\left(1+\frac{\gamma^2}{4}(\bar\alpha_0+\bar\alpha_1\cos 2\tau)+O(\gamma^4)\right)\\
\cos^2\mu\left(1+\frac{\gamma^2}{4}(\beta_0+\beta_1\cos 2\tau)\right) &= \frac{\cos^2\lambda\mu}{\lambda^2}\left(1+\frac{\gamma^2}{4}(\bar\beta_0+\bar\beta_1\cos 2\tau)+O(\gamma^4)\right)
\end{aligned}\tag{3.16}$$

where we introduce

$$\begin{aligned}
\kappa(\tau,\mu) &= 1-\frac{\gamma^2}{8}\left(\frac{21}{16}-\frac{3}{8}(1+2\cos^2\mu)\cos 2\tau\right)+O(\gamma^4)\\
\lambda(\tau,\mu) &= 1-\frac{\gamma^2}{8}\left(\frac{21}{16}+\frac{3}{4}\cos^2\mu-\frac{3}{8}\cos 2\tau\right)+O(\gamma^4)
\end{aligned}\tag{3.17}$$

One then finds

$$\begin{aligned}
\bar\alpha_0 &= \frac{1}{64}(1+6\cos 2\mu+5\cos 4\mu)\\
\bar\alpha_1 &= -\frac{1}{16}(5+\cos 4\mu-6(2+\cos 2\mu))+c_3\cos^2\mu\\
\bar\beta_0 &= c_2-\frac{21}{16}-\frac{1}{16}(25+16c_3)\cos^2\mu+\frac{3}{8}\cos^4\mu\\
\bar\beta_1 &= -\frac{1}{32}+\frac{c_3}{2}-\frac{5}{16}\cos 2\mu-\frac{3}{32}\cos 4\mu+\frac{3}{8}
\end{aligned}\tag{3.18}$$

JHEP06(2017)079

We now require that A and B have expansions

$$\frac{\cos^2\kappa\mu}{\kappa^2}\left(1+\frac{\gamma^2}{4}(\bar{\alpha}_0+\bar{\alpha}_1\cos 2\tau)+O(\gamma^4)\right)=(\mu-\mu_0)^2+O[\,(\mu-\mu_0)^3]$$
$$\frac{\cos^2\lambda\mu}{\lambda^2}\left(1+\frac{\gamma^2}{4}(\bar{\beta}_0+\bar{\beta}_1\cos 2\tau)+O(\gamma^4)\right)=(\mu-\mu_0)^2+O[\,(\mu-\mu_0)^3] \qquad (3.19)$$

near infinity with $\mu_0(\tau)=\frac{\pi}{2\kappa(\tau,\pi/2)}$. By comparing the coefficients of $(\mu-\mu_0)^2$, one may fix $c_2=\frac{21}{16}$ and $c_3=-\frac{9}{8}$. This choice fixes the freedom of coordinate scaling. Therefore one has

$$\begin{aligned}
\bar{\alpha}_0 &= -\frac{1}{16}\cos^2\mu(7-10\cos^2\mu)\\
\bar{\alpha}_1 &= \frac{1}{8}\cos^2\mu(1-4\cos^2\mu)\\
\bar{\beta}_0 &= -\frac{1}{16}\cos^2\mu(7-6\cos^2\mu)\\
\bar{\beta}_1 &= \frac{1}{8}\cos^2\mu(1-6\cos^2\mu)
\end{aligned} \qquad (3.20)$$

Thus

$$\begin{aligned}
\alpha_0 &= -\frac{1}{16}\cos^2\mu(7-10\cos^2\mu)+\frac{21}{16}(1+\mu\tan\mu)\\
\alpha_1 &= \frac{1}{8}\cos^2\mu(1-4\cos^2\mu)-\frac{3}{8}(1+2\cos^2\mu)(1+\mu\tan\mu)\\
\beta_0 &= -\frac{1}{16}\cos^2\mu(7-6\cos^2\mu)+\frac{1}{16}(21+12\cos^2\mu)(1+\mu\tan\mu)\\
\beta_1 &= \frac{1}{8}\cos^2\mu(1-6\cos^2\mu)-\frac{3}{8}(1+\mu\tan\mu)
\end{aligned} \qquad (3.21)$$

One further finds

$$\mu_0(\tau)=\frac{\pi}{2}\left[1+\frac{\gamma^2}{8}\left(\frac{21}{16}-\frac{3}{8}\cos 2\tau\right)+O(\gamma^4)\right] \qquad (3.22)$$

In this coordinate system, the (orbifold) singularity is still located at $\tau=\pm\frac{\pi}{2}$. Hence the τ directional coordinate is ranged over $[-\pi/2,\pi/2]$, which is the same as before. On the other hand, the spatial infinity is at $\mu=\pm\mu_0(\tau)$ so that the μ coordinate is ranged over

$$-\mu_0(\tau)\leq\mu\leq\mu_0(\tau) \qquad (3.23)$$

We depict the corresponding Penrose diagram of the perturbed BTZ black hole in figure 1. One finds the Penrose diagram is elongated horizontally in a τ-dependent manner. We find that any boundary two points cannot be connected by lightlike geodesics through the bulk including the present case as well as the cases discussed below. This in particular implies that the left and the right boundaries are causally disconnected completely. Hence there cannot be any interactions between the left and the right CFT's. We also find that $\mu_0(\tau)\geq\pi/2$ for all the cases considered below but we are not so sure if this holds in general.

JHEP06(2017)079

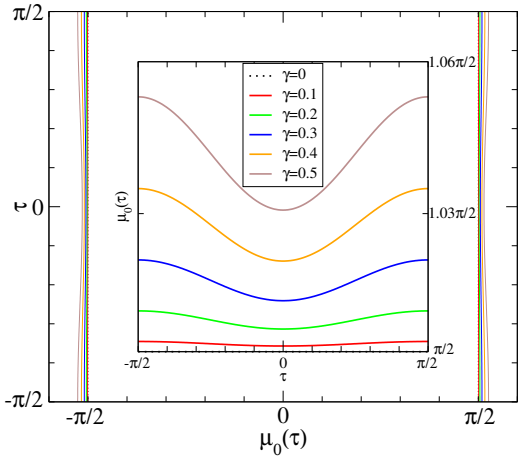

Figure 1. Penrose diagram of the perturbed BTZ black hole depicted for various γ. The relevant solution involves the scalar perturbation (3.12) with $m^2 = 0$.

3.2 Boundary stress tensor and horizon area

We let $O(t, \varphi)$ the operator dual to the scalar field ϕ. Then its vacuum expectation value may be identified as

$$\langle O(t,\varphi)\rangle = \frac{\gamma R^2}{8\pi G\ell^3}\frac{1}{\cosh^2\frac{tR}{\ell^2}}\tanh\frac{tR}{\ell^2} = \frac{\gamma\, c\pi}{3\beta^2}\frac{1}{\cosh^2\frac{2\pi t}{\beta}}\tanh\frac{2\pi t}{\beta} \tag{3.24}$$

where we used the standard holographic dictionary [11]. This shows exponential decaying behaviors. Here the temperature should be the late time equilibrium temperature since the system is time dependent. The perturbation may be characterized by the initial conditions

$$\begin{aligned}\langle O(0,\varphi)\rangle &= 0\\ \frac{\partial}{\partial t}\langle O(t,\varphi)\rangle|_{t=0} &= \frac{2c\pi^2}{3\beta^3}\gamma\end{aligned} \tag{3.25}$$

The initial perturbation are exponentially relaxed away in late time, which describes a thermalization of initial perturbation. The thermalization are controlled by the time scale

$$t_d = \frac{\beta}{2\pi} \tag{3.26}$$

Let us now show that the expression for the boundary stress tensor remains unperturbed. For this purpose, we shall construct asymptotic metric which is valid up to order $(\mu - \mu_0)^4$. Let us define $\bar{\mu}(\tau)$ by $\bar{\mu}(\tau) = \mu - \mu_0(\tau)$. The functions A and B can be expanded as

$$\begin{aligned}A &= \bar{\mu}^2\left(1 - \frac{1}{3}\bar{\mu}^2 + \frac{\gamma^2}{2}q\,\bar{\mu}\cos 2\tau + \cdots\right)\\ B &= \frac{\bar{\mu}^2}{\cos^2\tau}\left(1 - \frac{1}{3}\bar{\mu}^2 - \frac{\gamma^2}{2}q\,\bar{\mu} + \cdots\right)\end{aligned} \tag{3.27}$$

JHEP06(2017)079

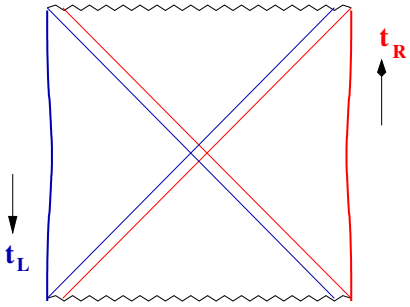

Figure 2. The future and past horizons are depicted by straight lines. The horizon length along the future horizon grows monotonically in time. The red lines are the horizons of the right side observer whereas the blue lines represent the horizons of the left side observer.

where $q = \frac{3\pi}{16}$ and $\cdots$ denotes higher order terms in $\bar{\mu}$ and γ. By the coordinate transformation,

$$\begin{aligned}\bar{\mu} &= \tilde{\mu} + \frac{\gamma^2}{4} q \cos 2\tilde{\tau} \sin^2 \tilde{\mu} + \cdots \\ \tau &= \tilde{\tau} + \frac{\gamma^2}{8} q \sin 2\tilde{\tau} \sin 2\tilde{\mu} + \cdots \end{aligned} \tag{3.28}$$

the metric becomes

$$\frac{ds^2}{\ell^2} = \frac{1}{\tilde{\mu}^2 \left(1 - \frac{1}{3}\tilde{\mu}^2 + \cdots\right)} \left[-d\tilde{\tau}^2 + d\tilde{\mu}^2 + \cos^2 \tilde{\tau}\, dx^2\right] \tag{3.29}$$

which agrees with the standard BTZ metric. Thus the stress energy tensor remains unchanged. The mass and pressure are then given by

$$M = 2\pi \ell\, p = \frac{1}{8G} \frac{R^2}{\ell^2} \tag{3.30}$$

which are time independent.

In figure 2, we draw the future and past horizons from the both boundaries. The horizons associated with the right/left boundary are depicted in red/blue color respectively. Let us now compute the horizon area along the right-side future horizon that is given by

$$\mu(\tau) = \tau - \frac{\pi}{2} + \mu_0\left(\frac{\pi}{2}\right) = \tau + \gamma^2 \frac{27\pi}{256} + O(\gamma^4) \tag{3.31}$$

The horizon area (length) becomes

$$\mathcal{A}(\tau) = 2\pi R \left[1 - \frac{\gamma^2}{128}\left(27 - 9\cos^2\tau + 22\cos^4\tau - 24\cos^6\tau - 27\left(\frac{\pi}{2} - \tau\right)\tan\tau\right) + O(\gamma^4)\right] \tag{3.32}$$

In the region near $\tau = -\frac{\pi}{2}$, our small γ approximation breaks down since the coefficient of γ^2 term becomes too large. In this region, one has to use $B(\tau, \mu)$ in (3.16) in the evaluation of $\mathcal{A}(\tau)$, from which one finds $\mathcal{A}(-\pi/2) = 0$ as expected. We draw the time dependence

JHEP06(2017)079

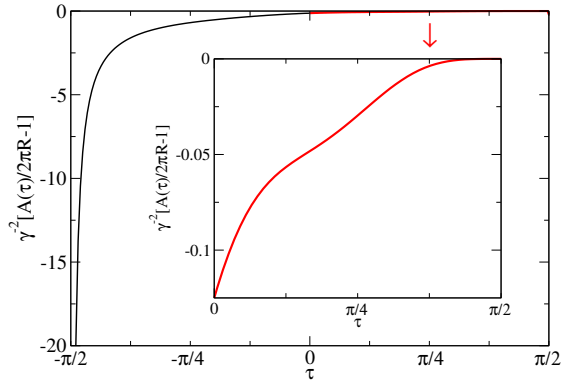

Figure 3. The future horizon area minus $2\pi R$ is depicted as a function of τ. In the region near $\tau = -\frac{\pi}{2}$, our small γ approximation breaks down since the coefficient of γ^2 term becomes too large. The validity requires that $|\mathcal{A}(\tau)/(2\pi R) - 1| \ll 1$.

of the horizon area in figure 3. One finds $\mathcal{A}(\pi/2)$ agrees with the BTZ value $2\pi R$ whereas $\mathcal{A}(0)$ is given by

$$\mathcal{A}(0) = 2\pi R\left[1 - \frac{\gamma^2}{8} + O(\gamma^4)\right] \tag{3.33}$$

The area is monotonically increasing as a function of time along the future horizon from zero to $2\pi R$. The corresponding entropy $S(\tau) = \mathcal{A}(\tau)/4G$ will be interpreted as a coarse-grained entropy of the system as discussed in detail in the next section.

3.3 Convenient form of coordinates

One may get a new coordinate system in which the form of the metric simplifies. For this we make the following coordinate transformation

$$\begin{aligned}\mu &= \sigma + \frac{3\gamma^2}{64}\left(\sigma\cos 2\sigma\cos 2\nu + \frac{7}{2}\sigma\right) + O(\gamma^4)\\ \tau &= \nu - \frac{3\gamma^2}{64}\left(\sigma\sin 2\sigma + \cos^2\sigma + \frac{1}{2}\right)\sin 2\nu + O(\gamma^4)\end{aligned} \tag{3.34}$$

Then the metric turns into the form

$$\frac{ds^2}{\ell^2} = \frac{1}{\cos^2\sigma}\left[-\frac{d\nu^2}{1+\frac{\gamma^2}{4}a_\nu + O(\gamma^4)} + \frac{d\sigma^2}{1+\frac{\gamma^2}{4}a_\sigma + O(\gamma^4)} + \frac{\cos^2\nu\, dx^2}{1+\frac{\gamma^2}{4}b_x + O(\gamma^4)}\right] \tag{3.35}$$

where

$$\begin{aligned}a_\sigma &= -\frac{1}{16}\cos^2\sigma(7 - 10\cos^2\sigma) - \frac{1}{8}\cos^2\sigma(11 + 4\cos^2\sigma)\cos 2\nu\\ a_\nu &= \frac{21}{16} - \frac{1}{16}\cos^2\sigma(7 - 10\cos^2\sigma) + \frac{1}{8}\cos^2\sigma(1 - 4\cos^2\sigma)\cos 2\nu\\ b_x &= \frac{18}{16} - \frac{1}{16}\cos^2\sigma(1 - 6\cos^2\sigma) + \frac{1}{16}\left(-3 + 4\cos^2\sigma(2 - 3\cos^2\sigma)\right)\cos 2\nu\end{aligned} \tag{3.36}$$

By further coordinate transformation, one may put b_x to zero but there seems no essential simplification in doing so. Note also that the entire Penrose diagram is covered by the coordinate ranges $\nu, \sigma \in [-\pi/2, \pi/2]$.

JHEP06(2017)079

4 Field theory construction

In the field theory side, initial states can be prepared following the thermofield construction in [6], which is generalized in [8]. Let us begin with general construction first. We insert operators along the Euclidean boundary, which deforms the field-theory Lagrangian by

$$\mathcal{L}(-it_E, \varphi) = \mathcal{L}_0(-it_E, \varphi) + \gamma g(t_E, \varphi) O(-it_E, \varphi) \tag{4.1}$$

where $t_E = it$ is the Euclidean boundary time that is circle compactified by

$$t_E \sim t_E + \beta \tag{4.2}$$

Here we choose t_E ranged over $[-\beta/2, \beta/2)$ and $g(t_E, \varphi)$ to satisfy the reflection positivity defined by

$$g^*(t_E, \varphi) = g(-t_E, \varphi) \tag{4.3}$$

assuming

$$O^\dagger(t, \varphi) = O(t, \varphi) \tag{4.4}$$

The Euclidean Lagrangian density is not real in general but the Euclidean action is real. Let $H(t_E)$ denote a corresponding Hamiltonian at Euclidean time t_E. Then the thermofield initial state is given by

$$|\psi(0,0)\rangle = \frac{1}{\sqrt{Z}} \sum_{mn} \langle n|U|m\rangle \ |\bar{m}\rangle_L \otimes |n\rangle_R \tag{4.5}$$

where Z is the normalization factor and $|\bar{m}\rangle$ denotes the state dual to $|m\rangle$. The operator U is in general given by

$$U = T \exp\left[- \int_{-\frac{\beta}{2}}^{0} dt_E H(t_E) \right] \tag{4.6}$$

The Lorentzian time evolution is given by the Hamiltonian

$$-H_L^T(t_L) \otimes 1 \, dt_L + 1 \otimes H_R(t_R) \, dt_R \tag{4.7}$$

where the left-right Hamiltonians are identified with

$$\begin{aligned} H_L(t_L) &= H\Big(- it_L - \frac{\beta}{2} \Big) \\ H_R(t_R) &= H\Big(it_R \Big) \end{aligned} \tag{4.8}$$

We associate the interval $[-\frac{\beta}{2}, -\frac{\beta}{4}) \oplus (\frac{\beta}{4}, \frac{\beta}{2}] \ / (-\frac{\beta}{4}, \frac{\beta}{4})$ to the Lorentzian time t_L/t_R of the left/right system by the analytic continuation where t_L/t_R is ranged over $(-\infty, \infty)$. This is depicted in the figure 4 where both the Euclidean and the Lorentzian geometry appear

JHEP06(2017)079

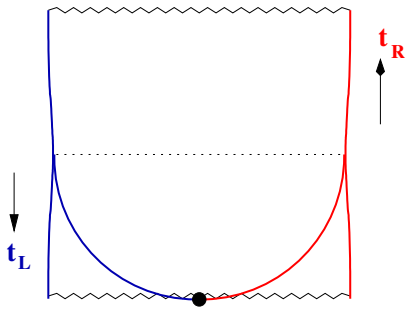

Figure 4. The combination of the Lorentzian and the Euclidean geometries is depicted. This is used to construct a thermofield initial state and subsequent Lorentzian time evolution.

at the same time. In this figure, we draw only the lower half of Euclidean evolution which is relevant to the initial ket state.

The red color is for the right side whereas the blue is for the left system. One can motivate the above choice in the following manner. Even with deformations, the coordinate transformation like (3.1) can be introduced for the asymptotic regions of the right and the left infinities. Then with $\mu = \pm\mu_0(\tau)$, one has the relations

$$\begin{aligned} \tanh\frac{2\pi}{\beta}t_R &= \sin\tau \\ \tanh\frac{2\pi}{\beta}t_L &= -\sin\tau \end{aligned} \tag{4.9}$$

which identifies the boundary times t_R and t_L. Since τ is ranged over $[-\frac{\pi}{2}, \frac{\pi}{2}]$, one sees that t_R and t_L are ranged over $(-\infty, \infty)$ as expected. Now by analytic continuation, the above becomes

$$\begin{aligned} \tan\frac{2\pi}{\beta}t_E^R &= \sinh\tau_E \\ \tan\frac{2\pi}{\beta}t_E^L &= -\sinh\tau_E \end{aligned} \tag{4.10}$$

where, from the Euclidean geometry, one finds that τ_E is ranged over $(-\infty, \infty)$. One finds that t_E^R can be chosen to be ranged over $(-\frac{\beta}{4}, \frac{\beta}{4})$ whereas t_E^L to be ranged over $[-\frac{\beta}{2}, -\frac{\beta}{4})\oplus(\frac{\beta}{4}, \frac{\beta}{2}]$. The right and the left parts cover the entire thermal circle in the end. Note that the points $t_E = \pm\frac{\beta}{4}$ is not associated with the right nor the left boundaries of the Lorentzian spacetime. Below we shall use these points to generate the state deformation without deforming the Hamiltonian.

As we already indicated, the identification of the Lorentzian Hamiltonian involves an analytic continuation from the Euclidean space. The lower half of the Euclidean solution covered by the interval $[-\frac{\beta}{2}, 0]$ is used to construct the thermofield initial state. Then the upper half is associated with the dual state of the thermofield state. This analytic continuation may not be allowed in general unless there is a further restriction on the form of $g(\tau_E, \varphi)$. For the Janus deformation in [8], one finds the analytic continuation indeed works. We leave further clarification of this issue to future works.

JHEP06(2017)079

Thus the time evolution is given by

$$|\psi(t_L,t_R)\rangle = T\exp\left[i\int_0^{t_L} dt'_L H_L^T(t'_L)\otimes 1\right] T\exp\left[-i\int_0^{t_R} dt'_R 1\otimes H_R(t'_R)\right]|\psi(0,0)\rangle \tag{4.11}$$

With this preliminary, let us consider an entanglement between the left and the right. For this, we introduce so called a reduced density matrix $\rho_R(t_R)$ defined by

$$\rho_R(t_R) = \mathrm{tr}_L|\psi(t_L,t_R)\rangle\langle\psi(t_L,t_R)| \tag{4.12}$$

where we trace over the left side Hilbert space. Then the entanglement entropy is defined by the von Neumann definition

$$S_R(t_R) = -\mathrm{tr}_R\rho_R(t_R)\log\rho_R(t_R) \tag{4.13}$$

This is in general time independent since $\rho_R(t_R)$ is related to $\rho_R(0)$ by $\mathcal{U}\,\rho_R(0)\,\mathcal{U}^\dagger$ with a unitary operator $\mathcal{U} = T\exp\left[-i\int_0^{t_R} dt'_R H_R(t'_R)\right]$. For the undeformed case with Hamiltonian H_0, one has $U = e^{-\frac{\beta}{2}H_0}$, which leads to $\rho_R = e^{-\beta H_0}/Z_0$. One gets the usual equilibrium thermodynamic entropy out of the entanglement entropy, which is describing the maximal entanglement of the left-right systems for a given temperature. The time-independence of (4.13) reflects that the right system alone evolves unitarily. Thus fine-grained information is fully preserved, which implies that the corresponding fine-grained (von Neumann) entropy should be time independent. In the above, however, we find that the horizon area grows. We interpret the corresponding horizon entropy as a coarse-grained entropy where the coarse-graining may be done by ignoring higher-order stringy interactions. In other words, there is a natural coarse-graining due to the gravity approximation that involves the small G (or large c) limit where especially the nonperturbative degrees are completely missing. These nonperturbative degrees include those of branes and various nonperturbative objects in string theory. In quantum field theory on $R\times S^1$, one may prove that there is a quantum Poincare recurrence theorem [12] saying that any initial vacuum expectation value of any operator should return within a Poincare recurrence time scale. Our gravity results violate the theorem, which is basically due to the above gravity approximation of large c limit. The fine-grained information is, of course, fully preserved and the coarse-graining due to the approximation is responsible for the violation of the theorem.

An expectation value obtained by insertion of the operator $O(t,\varphi)$ to the right side boundary is given by

$$\langle O(t,\varphi)\rangle = \langle\psi(0,0)|1\otimes O(t,\varphi)\,|\psi(0,0)\rangle \tag{4.14}$$

(Of course one may introduce a one-point function from the left boundary as well.) This can be evaluated perturbatively as

$$\langle O(t,\varphi)\rangle = \gamma\ell\int_{-\frac{\beta}{2}}^{\frac{\beta}{2}} ds\int_0^{2\pi} d\varphi' g(s,\varphi')\frac{1}{Z_0}\mathrm{tr}O(t,\varphi)O(-i(s-\pi),\varphi')e^{-\beta H_0} + O(\gamma^3) \tag{4.15}$$

JHEP06(2017)079

where H_0 is the undeformed CFT Hamiltonian. The two-point correlation function is given by

$$\frac{1}{Z_0}\mathrm{tr}O(t,\varphi)O(t',\varphi')e^{-\beta H_0}$$
$$=\frac{\ell^{d-1}d\Gamma(\Delta+)\left(\frac{\sqrt{2}\pi}{\beta}\right)^{2\Delta}}{8\pi^{\frac{d+2}{2}}G\,\Gamma\left(\Delta-\frac{d}{2}\right)}\sum_{m=-\infty}^{\infty}\frac{1}{\left[-\cosh\frac{2\pi}{\beta}(t-t')+\cosh\frac{2\pi\ell}{\beta}(\varphi-\varphi'+2\pi m)+i\epsilon\right]^{\Delta}} \tag{4.16}$$

in the AdS/CFT limit. Namely the expression is not exact but involves the large c gravity approximation. See [8, 13] for the normalization factor.

For the current problem, we consider the perturbation where $g(t_E,\varphi)$ is independent of φ with $\Delta=2$. The one point function then becomes

$$\langle O(t,\varphi)\rangle=\frac{\gamma\ell}{8\pi^2G}\left(\frac{2\pi}{\beta}\right)^3\int_{-\frac{\beta}{2}}^{\frac{\beta}{2}}ds\int_0^{\infty}dx\,g_0(s)\frac{1}{\left[-\cosh\frac{2\pi}{\beta}(t+is)+\cosh x\right]^2}+O(\gamma^3) \tag{4.17}$$

where $g(t_E,\varphi)=g_0(t_E)$. We compare this with the gravity computation in (3.24). Thus $g_0(s)$ can be determined by demanding

$$\int_{-\pi}^{\pi}du\int_0^{\infty}dx\,g_0\left(\frac{\beta u}{2\pi}\right)\frac{1}{\left[-\cosh(v+iu)+\cosh x\right]^2}=\frac{\pi}{\cosh^2 v}\tanh v \tag{4.18}$$

The function $g_0(z)$ is identified as

$$g_0(z)=-i\left[\delta\left(\frac{2\pi z}{\beta}-\frac{\pi}{2}\right)-\delta\left(\frac{2\pi z}{\beta}+\frac{\pi}{2}\right)\right] \tag{4.19}$$

which leads to $H_L(t)=H_R(t)=H_0$ that is the undeformed CFT Hamiltonian. In other words, the Hamiltonians remain intact under the perturbation (4.19) which inserts the operator precisely at $t_E=-\frac{\beta}{4}$. (There is, however, an example where the Lorentzian Hamiltonians are deformed [8].) Thus the Lorentzian evolution of the thermofield states simplifies as

$$|\psi(t_L,t_R)\rangle=e^{iH_0\otimes 1\,t_L-i1\otimes H_0\,t_R}|\psi(0,0)\rangle \tag{4.20}$$

On the other hand, the thermofield initial state $|\psi(0,0)\rangle$ is deformed because the operator U in (4.6) is modified to

$$U=e^{-\frac{\beta}{4}H_0}\,e^{i\gamma O_{200c}}\,e^{-\frac{\beta}{4}H_0}=e^{-\frac{\beta}{4}H_0}\,\left[1+i\gamma O_{200c}+\mathcal{O}(\gamma^2)\right]\,e^{-\frac{\beta}{4}H_0} \tag{4.21}$$

where $O_{\Delta njc}$ $(j\geq 0)$ and $O_{\Delta njs}$ $(j\geq 1)$ are defined by

$$O_{\Delta njc}=\frac{\ell\beta}{2\pi}\int_0^{2\pi}d\varphi\,\cos j\varphi\left(\frac{\beta}{2\pi}\frac{\partial}{\partial t}\right)^n O_\Delta(t,\varphi)|_{t=0}$$
$$O_{\Delta njs}=\frac{\ell\beta}{2\pi}\int_0^{2\pi}d\varphi\,\sin j\varphi\left(\frac{\beta}{2\pi}\frac{\partial}{\partial t}\right)^n O_\Delta(t,\varphi)|_{t=0} \tag{4.22}$$

Of course these kinds of definitions may be extended to arbitrary spin primary operators.

JHEP06(2017)079

It is clear that an operator insertion at $t_E = -\frac{\beta}{4}$ creates a deformation of state without deforming the left and the right Hamiltonians. In fact one may insert an arbitrary linear combination of operators

$$V = \sum_I C_I O_I \tag{4.23}$$

where O_I denote arbitrary linearly independent operators. Based on the operator state correspondence, this leads to rather general deformation of states without deforming the Hamiltonians of the system. In the next section we shall illustrate further gravity solutions corresponding to such deformation of states described in the above.

5 Other examples of micro-geometries

Other perturbation can be generated in many ways. Here we are interested only in the case where the boundary Hamiltonians are undeformed as in the previous section. One way to generate such perturbation is to choose $g(s, \varphi) = g_n(s)$ with

$$g_n(s) = \left(i \frac{\beta}{2\pi} \frac{d}{ds} \right)^n g_0(s) \tag{5.1}$$

The corresponding expectation value can be given by

$$\langle O(t, \varphi) \rangle_n = \left(\frac{\beta}{2\pi} \frac{\partial}{\partial t} \right)^n \langle O(t, \varphi) \rangle_0 + \mathcal{O}(\gamma^3) \tag{5.2}$$

which is derived from the formula (4.15). The scalar field solution can be generated similarly by

$$h_n(\tau, \mu) = \left(\frac{\beta}{2\pi} \frac{\partial}{\partial t} \right)^n h_0(\tau, \mu) \tag{5.3}$$

where the subscript 0 refers to our solution in section 3. This formula partly follows from the fact that the linearized scalar equation in (3.6) involves only coefficients which are independent of t when the equation is written in terms of coordinates (t, r, x). Thus partial derivatives with respect to t generate new solutions of the linearized equation in (3.6). For $n = 1$ case, one finds from the relation (3.1) that

$$h_1(\tau, \mu) = \gamma \cos^2 \mu \sin \mu (1 - 3 \sin^2 \tau) \tag{5.4}$$

and

$$\langle O(t, \varphi) \rangle_1 = \gamma \frac{c}{12\pi} \frac{R^2}{\ell^4} \frac{1}{\cosh^2 \frac{tR}{\ell^2}} \left[-2 + \frac{3}{\cosh^2 \frac{tR}{\ell^2}} \right] \tag{5.5}$$

The analysis of the corresponding back-reacted geometry is presented in appendix A. We obtain the deformation of the Penrose diagram which is again elongated horizontally. All the features of this solution are basically similar to those of the previous solution. In

JHEP06(2017)079

particular, this again describes the physics of thermalization though the detailed functional form is different from that of the previous solution.

Let us now consider an arbitrary linear combination of h_0 and h_1. Namely the linear combination

$$h(\tau,\mu) = \alpha_0\, h_0(\tau,\mu) + \alpha_1\, h_1(\tau,\mu) \tag{5.6}$$

solves the linearized scalar field equation in (3.7) where α_0 and α_1 are real. From this one may solve the linearized Einstein equations. Fortunately we do not have to solve the problem from the beginning. One finds

$$\begin{aligned} a(\tau,\mu) &= \alpha_0^2\, a_{200}(\tau,\mu) + \alpha_1^2\, a_{210}(\tau,\mu) + \alpha_0\alpha_1\, a_{201}(\tau,\mu) \\ b(\tau,\mu) &= \alpha_0^2\, b_{200}(\tau,\mu) + \alpha_1^2\, b_{210}(\tau,\mu) + \alpha_0\alpha_1\, b_{201}(\tau,\mu) \end{aligned} \tag{5.7}$$

where we use the notation $f_{\Delta n_1 n_2}(\tau,\mu)$. Here $n_2 = 0$ denotes that the solution of linearized Einstein equations is obtained with the scalar solution $h_{n_1}(\tau,\mu)$. On the other hand, the nonvanishing n_2 implies

$$f_{\Delta n_1 n_2}(\tau,\mu) = \left(\frac{\beta}{2\pi}\frac{\partial}{\partial t}\right)^{n_2} f_{\Delta n_1 0}(\tau,\mu) \tag{5.8}$$

Thus the cross terms follow from a_{200} and b_{200} by simply taking a derivative $\frac{\beta}{2\pi}\frac{\partial}{\partial t}$, which one may verify directly by solving the full equations of motion and fixing the homogeneous solutions. From the solution, again one can work out the field theory implications which are straightforward. Here let us just mention the shape of Penrose diagram which is dictated by $\mu_0^R(\tau)$ and $\mu_0^L(\tau)$ where μ is ranged over $[-\mu_0^L(\tau), \mu_0^R(\tau)]$. One finds that

$$\mu_0^{R/L}(\tau) = \frac{\pi}{2\kappa(\tau,\pi/2)} = 1 + \gamma^2 G^{R/L}(\tau) + O(\gamma^4) \tag{5.9}$$

with

$$\begin{aligned} G^{R/L}(\tau) = {} & \frac{\alpha_0^2}{8}\left(\frac{21}{16} - \frac{3}{8}\cos 2\tau\right) + \frac{3\alpha_1^2}{1024}(74 - 18\cos 2\tau + \cos 4\tau) \\ & \pm \frac{3\alpha_0\alpha_1}{128}\left(10\sin\tau + \sin 3\tau\right) \end{aligned} \tag{5.10}$$

where $\pm$ are for R and L respectively. We draw these functions in figure 5 to show the changes in the shape of the Penrose diagram. The shapes of the right boundary are illustrated for various α_0 and α_1 with $\alpha_0 = 1$. The shape of the left side is given by the relation $G^L(\alpha_0,\alpha_1) = G^R(\alpha_0,-\alpha_1)$.

There are further linearly independent perturbations with $m^2 = 0$. We choose the function $g(s)$ by

$$\bar{g}_0(s) = \delta\left(\frac{2\pi s}{\beta} - \frac{\pi}{2}\right) + \delta\left(\frac{2\pi s}{\beta} + \frac{\pi}{2}\right) \tag{5.11}$$

The corresponding scalar field reads

$$\bar{h}_0 = \frac{2}{\pi}\cos^2\mu\left(1 - \frac{1}{2}\log\left(\frac{1+\sin\tau}{1-\sin\tau}\right)\sin\tau\right) \tag{5.12}$$

JHEP06(2017)079

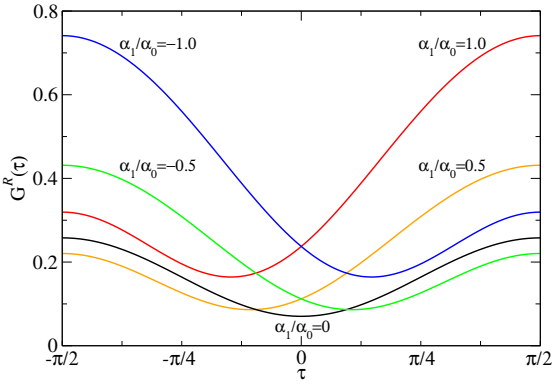

Figure 5. We depict here the boundary shapes given by $G^R(\alpha_0, \alpha_1)$ of the Penrose diagram of the spacetime with the linear combination of h_0 and h_1. We set $\alpha_0 = 1$ in the figure. The shape of the left side is given by the relation $G^L(\alpha_0, \alpha_1) = G^R(\alpha_0, -\alpha_1)$.

and the vev becomes

$$\langle O(t,\varphi)\rangle = \gamma \frac{c}{6\pi^2}\frac{R^2}{\ell^4}\frac{1}{\cosh^2\frac{tR}{\ell^2}}\left[1 - \frac{tR}{\ell^2}\tanh\frac{tR}{\ell^2}\right] \tag{5.13}$$

One may get the back-reacted solution for the gravity part but we find it is too complicated to present. The choice

$$g(s,\varphi) = \bar{g}_n(s) = \left(\frac{i\beta}{2\pi}\frac{d}{ds}\right)^n \bar{g}_0(s) \tag{5.14}$$

will also give the scalar solution given by

$$\bar{h}_n(\tau,\mu) = \left(\frac{\beta}{2\pi}\frac{\partial}{\partial t}\right)^n \bar{h}_0(\tau,\mu) \tag{5.15}$$

Finally we consider the case of massive scalar whose dual operator O_Δ has a general dimension Δ. The scalar equation (3.7) then has a simple solution in terms of Legendre functions,

$$h = \cos^\Delta\mu\,(\kappa_1 P_{\Delta-1}(\sin\tau) + \kappa_2 Q_{\Delta-1}(\sin\tau)) \tag{5.16}$$

Note that this reduces to (3.12) or (5.12) for massless case ($\Delta = 2$). Here we consider only the case with $\ell^2 m^2 = 3$ ($\Delta = 3$) and $\kappa_2 = 0$ for which the explicit form of the solution is given by

$$h = \cos^3\mu\left(-\frac{2}{3} + \cos^2\tau\right) \tag{5.17}$$

We present the corresponding back-reacted geometry explicitly in appendix B.

Let us now clarify the general structure of the Hilbert space of the boundary field theory and its realization in the gravity solution. For any Hermitian operator O_I constructed from some primary operator dual to the corresponding matter field in the gravity side, one may construct a rather general state by the insertion

$$U = e^{-\frac{\beta}{4}H_0}\left[1 + \gamma V + \mathcal{O}(\gamma^2)\right] e^{-\frac{\beta}{4}H_0} \tag{5.18}$$

JHEP06(2017)079

with $V = \sum_I C_I O_I$ where C_I are arbitrary complex numbers. For instance, for the operator O_{200}, one can choose the linear combination

$$g(s,\varphi) = \alpha_0\, g_0(s) + \bar{\alpha}_0\, \bar{g}_0(s) \tag{5.19}$$

which leads to

$$V = (\bar{\alpha}_0 + i\alpha_0) O_{200} = C_{200}\, O_{200} \tag{5.20}$$

where we take $\bar{\alpha}_I$ to be real. It is clear that the full Hilbert space of the underlying CFT is linearly realized by the inserted operator V. The realization of the leading order solution of matter part is unconventional though it is still linear. Namely one has

$$h = \alpha_0\, h_0 + \bar{\alpha}_0\, \bar{h}_0 \tag{5.21}$$

for the above example which does not realize the complex structure of the Hilbert space properly. Further the back-reaction of the gravity part is essentially nonlinear as is clear from the explicit solution (5.7). Hence we conclude that the AdS/CFT correspondence is not a linear correspondence in the sense that the linear structure of Hilbert space of the underlying CFT is realized nonlinearly in the gravity side. But we would like to emphasize that the gravity solution reflects all those information of the Hilbert space of the perturbative gravity description. As we discussed already, the gravity description misses the nonperturbative degrees such as branes and other nonperturbative objects in string theory.

6 Bulk dynamics

In this section, we shall discuss the behavior of the bulk field based on the above solutions. For an illustration, let us focus on the case of $m^2 = 0$ without the angular dependence on φ with $j = 0$. The most general solution in the leading order is given by

$$h(\tau,\mu) = \sum_{n=0}^{\infty} \left[\alpha_n\, h_n(\tau,\mu) + \bar{\alpha}_n\, \bar{h}_n(\tau,\mu)\right] \tag{6.1}$$

In order to cover the entire Penrose diagram which is deformed by perturbations, it is better to use the coordinates $(\nu,\sigma) \in [-\pi/2, \pi/2]^2$ that cover the entire Penrose diagram as introduced in section 3.3. Namely

$$h(\nu,\sigma) = h_e(\nu,\sigma) + \bar{h}_o(\nu,\sigma) \tag{6.2}$$

with

$$h_e(\nu,\sigma) = \sum_{n=0}^{\infty} \bar{\alpha}_n\, \bar{h}_n(\nu,\sigma) \ , \quad h_o(\nu,\sigma) = \sum_{n=0}^{\infty} \alpha_n\, h_n(\nu,\sigma) \tag{6.3}$$

gives a solution fully covering the deformed Penrose diagram which is also valid to the leading order since the correction due to geometry gives $\mathcal{O}(\gamma^3)$ contributions. We shall discuss properties of this solution. First of all, there is a symmetry

$$\begin{aligned} h_n(-\nu,-\sigma) &= -h_n(\nu,\sigma) \\ \bar{h}_n(-\nu,-\sigma) &= \bar{h}_n(\nu,\sigma) \end{aligned} \tag{6.4}$$

which leads to the symmetry of the solution

$$\begin{aligned} h_o(-\nu,-\sigma) &= -h_o(\nu,\sigma) \\ h_e(-\nu,-\sigma) &= h_e(\nu,\sigma) \end{aligned} \tag{6.5}$$

This symmetry basically follows from the symmetry of the BTZ background and our choice of the thermofield initial state. The perturbation satisfies the spatial boundary condition $h(\nu,\pm\pi/2) = 0$, which is our choice since there are examples [7, 8, 14] for which this condition is relaxed. Now we shall give an initial condition at $\nu = 0$ by

$$\begin{aligned} h(0,\sigma) &= q_1(\sigma) \\ \partial_\nu h(\nu,\sigma)|_{\nu=0} &= q_2(\sigma) \end{aligned} \tag{6.6}$$

We illustrate this bulk perturbative dynamics in figure 6, where the left and the right initial perturbations can be independent from each other. Note that the set

$$\{h_{2n+1}(0,\sigma)/\cos\sigma,\ \bar{h}_{2n}(0,\sigma)/\cos\sigma \mid n = 0,1,2,\cdots\} \tag{6.7}$$

forms a complete basis satisfying Dirichlet boundary condition for the interval $\sigma \in [-\pi/2,\pi/2]$. Hence $q_1(\sigma) = \cos\sigma f_1(\sigma)$ where $f_1(\sigma)$ is an arbitrary real function satisfying the Dirichlet boundary condition. The $\cos\sigma$ factor here follows from the fact that we are considering the bulk field dual to the dimension two operator. Similarly $q_2(\sigma) = \cos\sigma f_2(\sigma)$ where $f_2(\sigma)$ is an arbitrary real function satisfying the Dirichlet boundary condition where now the basis is given by

$$\{\partial_\nu h_{2n}(\nu,\sigma)|_{\nu=0}/\cos\sigma,\ \partial_\nu \bar{h}_{2n+1}(\nu,\sigma)|_{\nu=0}/\cos\sigma \mid n = 0,1,2,\cdots\} \tag{6.8}$$

Thus we find that the initial configuration together with the velocity can be fully localized in the bulk once it satisfies the boundary condition. In particular one can choose initial conditions such that it can be fully localized behind the horizon. The subsequent ν development is determined by the wave equation in (3.7) which is defined in the fully extended BTZ spacetime. The time evolution is well defined except the divergence at the orbifold singularities $\nu = \pm\pi/2$ where $\bar{h}_n$ diverges. These are associated with the problems of the singularities behind horizon, to which we have nothing to add in this note. (As will be argued below, our gravity description fails near $\tau = \pm\pi/2$ where the singularity is located.) Their features are not different from those of cosmological singularities in the sense that the singularities are spacelike. Away from $\nu = \pm\pi/2$, its time evolution is ordinary. In particular nothing special happens near horizon regions.

Now we would like to discuss the decoding of information in relation with the above setup. We shall discuss the problem from the viewpoint of the observer of the right boundary. The information we are interested in is contained in the coefficients $(\alpha_n, \bar{\alpha}_n)$. There is no subtlety in this bulk description since the simple wave equation governs this reduced information content of the system. There are three levels of available descriptions. First is the description in terms of the solution (6.2) of the wave equation (3.7). The second is the full gravity description allowing back-reactions, which is coarse-grained from the viewpoint

JHEP06(2017)079

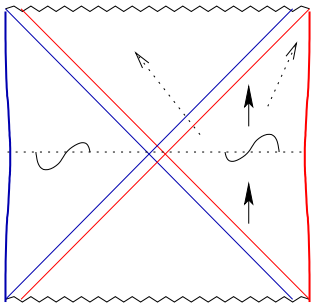

Figure 6. We illustrate here the bulk perturbative dynamics. The initial condition is given at $\nu = 0$. The left and the right initial perturbations can be independent from each other. The dotted lines with an arrow represent possible bulk observer's trajectories. All the information they can gather lies in the right side of horizons that are colored in red.

of the full microscopic degrees as we discussed before. Finally there is the full microscopic description by the boundary field theory. In particular $\rho_R(t_R)$ contains all those microscopic information available from the viewpoint of an observer on the right boundary. This will require the full string theory from the viewpoint of the bulk. As we demonstrated already, the information contained in ρ_R does not change in time and hence all the initial information is preserved in time. On the other hand, at the level of gravity description, one finds the future horizon area grows which we also demonstrated already. Hence for the bulk observer staying outside the future horizon, the less region of σ is available observationally. The observer is then able to determine less information on the coefficients $(\alpha_n, \bar{\alpha}_n)$ as the horizon area grows. Hence the information seems to disappear from the bulk observer at this linearized level. The observer may jump into the black hole interior. But he cannot cross the past horizon of the right side, which is the $-45°$ red line in figure 6. Hence one seems to find again less information available since the bigger region is excluded from observation. The semiclassical treatment does not help either since the problem is basically from the causality imposed by the horizon.

Note however that the effect is of order γ^2 since missing information is mainly due to the horizon change that is of order γ^2. The higher order contributions including gravity back-reaction help here which can contain the missing information. (If we know all of $(\alpha_n, \bar{\alpha}_n)$ for instance, the higher order contributions give completely redundant information on $(\alpha_n, \bar{\alpha}_n)$.) There are other ways to argue the recovery of information by the higher order effects. One considers the coupling of the left-right boundary by the double trace deformation [15]. Then this makes Penrose diagram contracted instead of elongation which leads to an effective reduction of the horizon area. Hence this way one may recover the missing perturbative information at the level of wave equation. Therefore all the information regarding the perturbative gravity fluctuation may be restored.

On the other hand, we have demonstrated that, within the gravity description, the expectation value of operator decays exponentially in time violating the Poincare recurrence theorem. This in particular implies that the gravity description is not valid at $t = \pm\infty$ (or $\tau = \pm\pi/2$) where we set out initial state at $t = 0$. Thus the missing information at the

JHEP06(2017)079

microscopic level should lie in the degrees that are responsible for the dynamics beyond gravity approximation. These degrees are coarse-grained within the gravity description. Their dynamics are nonperturbative in the sense that we do not have a well-defined geometric description of micro-geometries.

This shows that the information loss cannot be resolved within the perturbative gravity framework even if one includes its perturbative back-reactions. We do not know how the missing information is stored in such nonperturbative degrees.

7 Conclusions

In this note we have considered the deformation of BTZ black holes in the context of AdS/CFT correspondence. The geometry is dual to a deformation of thermofield initial state while the boundary Hamiltonians remain intact. To deform initial states, we insert a generic linear combination of operators to the mid-point of the Euclidean time evolution which is used to construct the thermofield initial states. For each insertion, we can construct the corresponding back-reacted geometries. The corresponding geometries encode the information of the CFT side though their relation is highly nonlinear. The resulting geometries describe the exponential relaxation of any initial perturbation above the thermal vacuum, which is the thermalization of any initial perturbation.

Our construction of the micro geometries has many potential applications. One may compute for instance multi-point functions from our geometry. Especially evaluation of the out-of-time-order 4-point function [16] that shows the quantum chaos behavior [17] is rather straightforward. Here we expect one can compute the behavior of the 4-point function that is valid for entire range of time without any further restriction. This 4-point function involves an insertion of operators from the both boundaries at the same time. One finds that the behind-horizon degrees are relevant in the evaluation of the 4-point function. We will report the related study elsewhere.

Our construction of micro-thermofield geometries are different from the fuzzball proposal [18] in many ways. First of all our construction is entirely based on the standard AdS/CFT correspondence. Our micro geometries do not involve any particular bulk local structures on which the fuzzball proposal is based on. Moreover, our deformation always involves black hole horizon though it is not entirely clear whether the existence of horizon is a necessary condition or not. Of course one still has a pure state description from the viewpoint of the total system of the both boundaries. This is sharply contrasted with the fuzzball proposal where the existence of any horizon in the bulk is disputed.

Acknowledgments

We would like to thank Hyunsoo Min for his contribution at the early stage of this work. D.B. was supported in part by NRF Grant 2017R1A2B4003095. K.K. was supported by NRF Grant 2015R1D1A1A01058220 and by the faculty research fund of Sejong University in 2017.

JHEP06(2017)079

A Other perturbation with $m^2 = 0$

For $n = 1$ case, one has

$$h_1 = \gamma \cos^2\mu \sin\mu(1 - 3\sin^2\tau) \tag{A.1}$$

Following section 3, we can find the corresponding perturbation for the gravity part in the form

$$\begin{aligned} A &= \cos^2\mu\left(1 + \frac{\gamma^2}{4}a\right) = \frac{\cos^2\kappa\mu}{\kappa^2}\left(1 + \frac{\gamma^2}{4}\bar{a}\right) = (\mu - \mu_0)^2 + O[(\mu - \mu_0)^3] \\ B &= \frac{\cos^2\mu}{\cos^2\tau}\left(1 + \frac{\gamma^2}{4}b\right) = \frac{\cos^2\lambda\mu}{\lambda^2\cos^2\tau}\left(1 + \frac{\gamma^2}{4}\bar{b}\right) = \frac{(\mu - \mu_0)^2}{\cos^2\tau} + O[(\mu - \mu_0)^3] \end{aligned} \tag{A.2}$$

where

$$\begin{aligned} a &= \alpha_0(\mu) + \alpha_1(\mu)\cos 2\tau + \alpha_2(\mu)\cos 4\tau \\ b &= \beta_0(\mu) + \beta_1(\mu)\cos 2\tau + \beta_2(\mu)\cos 4\tau \end{aligned} \tag{A.3}$$

with

$$\begin{aligned} \alpha_0 &= \frac{1}{64}(111 - 37\cos^2\mu + 126\cos^4\mu - 120\cos^6\mu) + \frac{111}{64}\mu\tan\mu \\ \alpha_1 &= -\frac{3}{64}(9 + 15\cos^2\mu + 44\cos^4\mu - 36\cos^6\mu) - \frac{27}{64}\mu(1 + 2\cos\mu^2)\tan\mu \\ \alpha_2 &= \frac{1}{128}(3 + 23\cos^2\mu + 150\cos^4\mu - 144\cos^6\mu) + \frac{1}{128}\mu(3 + 24\cos\mu^2 - 72\cos^4\mu)\tan\mu \\ \beta_0 &= \frac{1}{64}(111 + 23\cos\mu^2 + 94\cos^4\mu - 60\cos^6\mu) + \frac{3}{64}\mu(37 + 20\cos\mu^2 - 4\cos^4\mu)\tan\mu \\ \beta_1 &= -\frac{1}{64}(27 + 3\cos\mu^2 + 122\cos^4\mu - 120\cos^6\mu) - \frac{3}{64}\mu(9 + 4\cos\mu^2 - 8\cos^4\mu)\tan\mu \\ \beta_2 &= \frac{1}{128}(3 - 13\cos\mu^2 + 234\cos^4\mu - 240\cos^6\mu) + \frac{3}{128}\mu(1 - 4\cos\mu^2)\tan\mu \end{aligned} \tag{A.4}$$

Also

$$\begin{aligned} \kappa &= 1 - \frac{3}{1024}\gamma^2[74 - 18(1 + 2\cos^2\mu)\cos 2\tau + (1 + 8\cos^2\mu - 24\cos^4\mu)\cos 4\tau] + O(\gamma^4) \\ \lambda &= 1 - \frac{3}{1024}\gamma^2[74 + 40\cos^2\mu - 8\cos^4\mu + 2(-9 - 4\cos^2\mu + 8\cos^4\mu)\cos 2\tau \\ &\qquad + (1 - 4\cos^2\mu)\cos 4\tau] + O(\gamma^4) \end{aligned} \tag{A.5}$$

and

$$\begin{aligned} \bar{a} &= \bar{\alpha}_0(\mu) + \bar{\alpha}_1(\mu)\cos 2\tau + \bar{\alpha}_2(\mu)\cos 4\tau \\ \bar{b} &= \bar{\beta}_0(\mu) + \bar{\beta}_1(\mu)\cos 2\tau + \bar{\beta}_2(\mu)\cos 4\tau \end{aligned} \tag{A.6}$$

JHEP06(2017)079

with

$$\begin{aligned}
\bar{\alpha}_0 &= -\frac{1}{64}\cos^2\mu(37-126\cos^2\mu+120\cos^4\mu)\\
\bar{\alpha}_1 &= \frac{3}{64}\cos^2\mu(3-44\cos^2\mu+36\cos^4\mu)\\
\bar{\alpha}_2 &= -\frac{1}{128}\cos^2\mu(1-222\cos^2\mu+144\cos^4\mu)\\
\bar{\beta}_0 &= -\frac{1}{64}\cos^2\mu(37-106\cos^2\mu+60\cos^4\mu)\\
\bar{\beta}_1 &= \frac{1}{64}\cos^2\mu(9-146\cos^2\mu+120\cos^4\mu)\\
\bar{\beta}_2 &= -\frac{1}{128}\cos^2\mu(1-234\cos^2\mu+240\cos^4\mu)
\end{aligned} \tag{A.7}$$

and

$$\mu_0(\tau)=\frac{\pi}{2\kappa(\pi/2,\tau)}=\frac{\pi}{2}\left(1+\frac{3}{1024}\gamma^2(74-18\cos 2\tau+\cos 4\tau)+O(\gamma^4)\right) \tag{A.8}$$

The function $\mu_0(\tau)$ has the similar shape to figure 1. We draw the deformation of the Penrose diagram in figure 7. As in section 3.2, the metric can be transformed to the standard BTZ metric (3.29) by the coordinate transformation,

$$\begin{aligned}
\bar{\mu} &= \tilde{\mu}+\frac{3\pi\gamma^2}{512}\sin^2\tilde{\mu}(9\cos 2\tilde{\tau}-2\cos 4\tilde{\tau})+\cdots\\
\tau &= \tilde{\tau}+\frac{3\pi\gamma^2}{1024}(9\sin 2\tilde{\mu}-\sin 4\tilde{\mu}\cos 2\tilde{\tau})\sin 2\tilde{\tau}+\cdots
\end{aligned} \tag{A.9}$$

Along the future horizon

$$\mu=\tau-\frac{\pi}{2}+\mu_0\left(\frac{\pi}{2}\right)=\tau+\gamma^2\frac{279\pi}{2048}+O(\gamma^4) \tag{A.10}$$

the horizon length is a monotonically increasing function

$$\begin{aligned}
\mathcal{A}(\tau)=2\pi R\Bigg[1+\frac{\gamma^2}{1024}\Bigg(&-279+93\cos^2\tau-782\cos^4\tau+3064\cos^6\tau-4272\cos^8\tau\\
&+1920\cos^{10}\tau+279\left(\frac{\pi}{2}-\tau\right)\tan\tau\Bigg)+O(\gamma^4)\Bigg]
\end{aligned} \tag{A.11}$$

Then $\mathcal{A}(\pi/2)=2\pi R$ which is the BTZ value while $\mathcal{A}(0)$ is given by

$$\mathcal{A}(0)=2\pi R\left[1-\frac{\gamma^2}{4}+O(\gamma^4)\right] \tag{A.12}$$

A coordinate transformation

$$\begin{aligned}
\tau &= \nu-\frac{3\gamma^2}{4096}[36\sin 2\nu(\cos 2\sigma+2\sigma\sin 2\sigma)+\sin 4\nu(\cos 4\sigma+4\sigma\sin 4\sigma)]\\
\mu &= \sigma+\frac{3\gamma^2}{1024}\sigma(74+18\cos 2\nu\cos 2\sigma+\cos 4\nu\cos 4\sigma)
\end{aligned} \tag{A.13}$$

JHEP06(2017)079

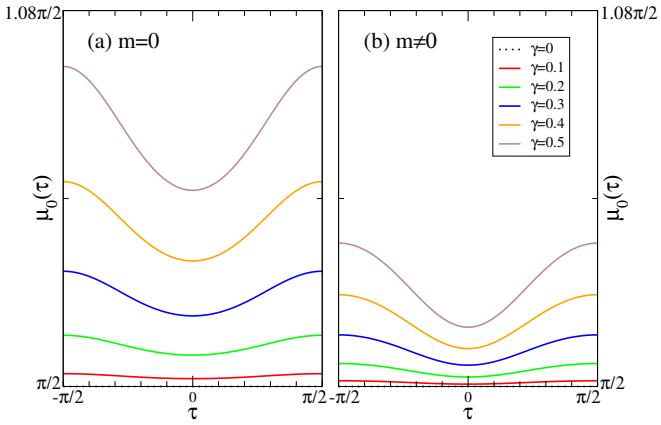

Figure 7. Penrose diagrams of the perturbed BTZ black hole. (a) $m = 0$ with the perturbation (A.1) (b) $m = \sqrt{3}/\ell$ with the perturbation (B.1).

gives the metric of the form (3.35) with

$$\begin{aligned}
a_\nu = \frac{1}{128}[&222 - 74\cos^2\sigma + 252\cos^4\sigma - 240\cos\sigma^6 \\
&+ 6\cos 2\nu(-18 + 3\cos^2\sigma - 44\cos^4\sigma + 36\cos^6\sigma) \\
&- \cos 4\nu(-6 + \cos^2\sigma - 174\cos^4\sigma + 144\cos^6\sigma)] \\
a_\sigma = -\frac{1}{128}\cos^2\sigma[&74 - 252\cos^2\sigma + 240\cos^4\sigma \\
&+ 6\cos 2\nu(33 + 44\cos^2\sigma - 36\cos^4\sigma) \\
&+ \cos 4\nu(-47 + 18\cos^2\sigma(-7 + 8\cos^2\sigma)] \\
b_x = \frac{1}{512}[&999 - 8\cos^2\sigma(7 - 97\cos^2\sigma + 60\cos^4\sigma) \\
&- \cos 2\nu(330 - 16\cos^2\sigma(15 - 64\cos^2\sigma + 60\cos^4\sigma)) \\
&- \cos 4\nu(-15 + 76\cos^2\sigma - 960\cos^4\sigma + 960\cos^6\sigma)]
\end{aligned} \tag{A.14}$$

B Other perturbation with $m^2 \neq 0$

Here we consider only the case with $\ell^2 m^2 = 3$ ($\Delta = 3$) and $\kappa_2 = 0$ in (5.16) for which the explicit form of the solution is given by

$$h = \cos^3\mu\left(-\frac{2}{3} + \cos^2\tau\right) \tag{B.1}$$

The corresponding solution in the gravity part can be obtained in the form (A.2) and (A.3) with

$$\begin{aligned}
\alpha_0 &= \frac{1}{192}(135 - 45\cos^2\mu - 18\cos^4\mu + 40\cos^6\mu) + \frac{45}{64}\mu\tan\mu \\
\alpha_1 &= -\frac{1}{576}(165 + 275\cos^2\mu - 132\cos^4\mu + 108\cos^6\mu) - \frac{55}{192}\mu(1 + 2\cos\mu^2)\tan\mu \\
\alpha_2 &= -\frac{1}{1152}(15 + 115\cos^2\mu - 402\cos^4\mu - 144\cos^6\mu) \\
&\quad - \frac{5}{384}\mu(1 + 8\cos\mu^2 - 24\cos^4\mu)\tan\mu
\end{aligned}$$

JHEP06(2017)079

$$
\begin{aligned}
\beta_0 &= \frac{1}{576}(405 + 165\cos^2\mu - 94\cos^4\mu + 60\cos^6\mu) \\
&\quad + \frac{5}{192}\mu(27 + 20\cos^2\mu + 4\cos^4\mu)\tan\mu \\
\beta_1 &= -\frac{1}{576}(165 - 115\cos^2\mu + 118\cos^4\mu + 120\cos^6\mu) \\
&\quad - \frac{5}{192}\mu(11 - 4\cos^2\mu + 8\cos^4\mu)\tan\mu \\
\beta_2 &= -\frac{1}{1152}(15 - 65\cos\mu^2 + 18\cos^4\mu - 240\cos^6\mu) - \frac{5}{384}\mu(1 - 4\cos\mu^2)\tan\mu
\end{aligned} \tag{B.2}
$$

Also

$$
\begin{aligned}
\kappa &= 1 - \frac{5}{3072}\gamma^2[54 - 22(1 + 2\cos^2\mu)\cos 2\tau - (1 + 8\cos^2\mu - 24\cos^4\mu)\cos 4\tau] + O(\gamma^4) \\
\lambda &= 1 - \frac{5}{3072}\gamma^2[54 + 40\cos^2\mu + 8\cos^4\mu - (22 - 8\cos^2\mu + 16\cos^4\mu)\cos 2\tau \\
&\qquad - (1 - 4\cos^2\mu)\cos 4\tau] + O(\gamma^4)
\end{aligned} \tag{B.3}
$$

and

$$
\begin{aligned}
\bar{a} &= \bar{\alpha}_0(\mu) + \bar{\alpha}_1(\mu)\cos 2\tau + \bar{\alpha}_2(\mu)\cos 4\tau \\
\bar{b} &= \bar{\beta}_0(\mu) + \bar{\beta}_1(\mu)\cos 2\tau + \bar{\beta}_2(\mu)\cos 4\tau
\end{aligned} \tag{B.4}
$$

with

$$
\begin{aligned}
\bar{\alpha}_0 &= -\frac{1}{192}\cos^2\mu(45 + 18\cos^2\mu - 40\cos^4\mu) \\
\bar{\alpha}_1 &= \frac{1}{576}\cos^2\mu(55 + 132\cos^2\mu - 108\cos^4\mu) \\
\bar{\alpha}_2 &= \frac{1}{1152}\cos^2\mu(5 + 42\cos^2\mu + 144\cos^4\mu) \\
\bar{\beta}_0 &= -\frac{1}{576}\cos^2\mu(135 + 154\cos^2\mu - 60\cos^4\mu) \\
\bar{\beta}_1 &= \frac{1}{576}\cos^2\mu(55 + 2\cos^2\mu - 120\cos^4\mu) \\
\bar{\beta}_2 &= \frac{1}{1152}\cos^2\mu(5 - 18\cos^2\mu + 240\cos^4\mu)
\end{aligned} \tag{B.5}
$$

and

$$
\mu_0(\tau) = \frac{\pi}{2\kappa(\pi/2,\tau)} = \frac{\pi}{2}\left(1 + \frac{5}{3072}\gamma^2(54 - 22\cos 2\tau - \cos 4\tau) + O(\gamma^4)\right) \tag{B.6}
$$

We draw the shape of the Penrose diagram on the right side of figure 7. The metric can again be transformed to the standard BTZ metric (3.29) by the coordinate transformation,

$$
\begin{aligned}
\bar{\mu} &= \tilde{\mu} + \frac{5\pi\gamma^2}{1536}\sin^2\tilde{\mu}(11\cos 2\tilde{\tau} + 2\cos 4\tilde{\tau}) + \cdots \\
\tau &= \tilde{\tau} + \frac{5\pi\gamma^2}{3072}(11\sin 2\tilde{\mu} + \sin 4\tilde{\mu}\cos 2\tilde{\tau})\sin 2\tilde{\tau} + \cdots
\end{aligned} \tag{B.7}
$$

JHEP06(2017)079

Along the future horizon

$$\mu = \tau - \frac{\pi}{2} + \mu_0\left(\frac{\pi}{2}\right) = \tau + \gamma^2\frac{125\pi}{2048} + O(\gamma^4) \tag{B.8}$$

the horizon length becomes again a monotonically increasing function

$$\begin{aligned}\mathcal{A}(\tau) = 2\pi R\Big[1 + \frac{\gamma^2}{3072}\Big(&-375 + 125\cos^2\tau + 50\cos^4\tau - 264\cos^6\tau + 848\cos^8\tau \\ &- 640\cos^{10}\tau + 375\Big(\frac{\pi}{2} - \tau\Big)\tan\tau\Big) + O(\gamma^4)\Big]\end{aligned} \tag{B.9}$$

Then $\mathcal{A}(\pi/2) = 2\pi R$ which is the BTZ value as before while $\mathcal{A}(0)$ is given by

$$\mathcal{A}(0) = 2\pi R\left[1 - \frac{\gamma^2}{12} + O(\gamma^4)\right] \tag{B.10}$$

A coordinate transformation

$$\begin{aligned}\tau &= \nu - \frac{5\gamma^2}{12288}[44\sin 2\nu(\cos 2\sigma + 2\sigma\sin 2\sigma) - \sin 4\nu(\cos 4\sigma + 4\sigma\sin 4\sigma)] \\ \mu &= \sigma + \frac{5\gamma^2}{3072}\sigma(54 + 22\cos 2\nu\cos 2\sigma - \cos 4\nu\cos 4\sigma)\end{aligned} \tag{B.11}$$

gives the metric of the form (3.35) with

$$\begin{aligned}a_\nu &= \frac{1}{1152}[6(135 - 45\cos^2\sigma - 18\cos^4\sigma + 40\cos\sigma^6) \\ &\quad + \cos 2\nu(-660 + 110\cos^2\sigma + 264\cos^4\sigma - 216\cos^6\sigma) \\ &\quad + \cos 4\nu(-30 + 5\cos^2\sigma + 282\cos^4\sigma + 144\cos^6\sigma)] \\ a_\sigma &= -\frac{1}{1152}\cos^2\sigma[6(45 + 18\cos^2\sigma - 40\cos^4\sigma) \\ &\quad + 2\cos 2\nu(605 - 132\cos^2\sigma + 108\cos^4\sigma) \\ &\quad + \cos 4\nu(235 - 18\cos^2\sigma(29 + 8\cos^2\sigma)] \\ b_x &= \frac{1}{4608}[3885 + 120\cos^2\sigma - 872\cos^4\sigma + 480\cos^6\sigma \\ &\quad - 2\cos 2\nu(975 + 8\cos^2\sigma(-125 + 44\cos^2\sigma + 60\cos^4\sigma)) \\ &\quad - \cos 4\nu(75 - 380\cos^2\sigma + 192\cos^4\sigma - 960\cos^6\sigma)]\end{aligned} \tag{B.12}$$

References

[1] J.M. Maldacena, *The large-N limit of superconformal field theories and supergravity*, *Int. J. Theor. Phys.* **38** (1999) 1113 [*Adv. Theor. Math. Phys.* **2** (1998) 231] [hep-th/9711200] [INSPIRE].

[2] S.S. Gubser, I.R. Klebanov and A.M. Polyakov, *Gauge theory correlators from noncritical string theory*, *Phys. Lett.* **B 428** (1998) 105 [hep-th/9802109] [INSPIRE].

JHEP06(2017)079

[3] E. Witten, *Anti-de Sitter space and holography*, *Adv. Theor. Math. Phys.* **2** (1998) 253 [hep-th/9802150] [INSPIRE].

[4] M. Bañados, C. Teitelboim and J. Zanelli, *The black hole in three-dimensional space-time*, *Phys. Rev. Lett.* **69** (1992) 1849 [hep-th/9204099] [INSPIRE].

[5] Y. Takahasi and H. Umezawa, *Thermo field dynamics*, *Collect. Phenom.* **2** (1975) 55 [INSPIRE].

[6] J.M. Maldacena, *Eternal black holes in Anti-de Sitter*, *JHEP* **04** (2003) 021 [hep-th/0106112] [INSPIRE].

[7] D. Bak, M. Gutperle and S. Hirano, *Three dimensional Janus and time-dependent black holes*, *JHEP* **02** (2007) 068 [hep-th/0701108] [INSPIRE].

[8] D. Bak, M. Gutperle and A. Karch, *Time dependent black holes and thermal equilibration*, *JHEP* **12** (2007) 034 [arXiv:0708.3691] [INSPIRE].

[9] D. Bak, M. Gutperle and S. Hirano, *A dilatonic deformation of AdS_5 and its field theory dual*, *JHEP* **05** (2003) 072 [hep-th/0304129] [INSPIRE].

[10] J. de Boer, *Six-dimensional supergravity on $S^3 \times AdS_3$ and 2D conformal field theory*, *Nucl. Phys.* **B 548** (1999) 139 [hep-th/9806104] [INSPIRE].

[11] K. Skenderis, *Lecture notes on holographic renormalization*, *Class. Quant. Grav.* **19** (2002) 5849 [hep-th/0209067] [INSPIRE].

[12] L. Dyson, M. Kleban and L. Susskind, *Disturbing implications of a cosmological constant*, *JHEP* **10** (2002) 011 [hep-th/0208013] [INSPIRE].

[13] D. Bak, *Information metric and Euclidean Janus correspondence*, *Phys. Lett.* **B 756** (2016) 200 [arXiv:1512.04735] [INSPIRE].

[14] D. Bak, M. Gutperle and R.A. Janik, *Janus black holes*, *JHEP* **10** (2011) 056 [arXiv:1109.2736] [INSPIRE].

[15] P. Gao, D.L. Jafferis and A. Wall, *Traversable wormholes via a double trace deformation*, arXiv:1608.05687 [INSPIRE].

[16] J. Maldacena, S.H. Shenker and D. Stanford, *A bound on chaos*, *JHEP* **08** (2016) 106 [arXiv:1503.01409] [INSPIRE].

[17] S.H. Shenker and D. Stanford, *Black holes and the butterfly effect*, *JHEP* **03** (2014) 067 [arXiv:1306.0622] [INSPIRE].

[18] S.D. Mathur, *The fuzzball proposal for black holes: an elementary review*, *Fortsch. Phys.* **53** (2005) 793 [hep-th/0502050] [INSPIRE].

[19] K. Goto and T. Takayanagi, *CFT descriptions of bulk local states in the AdS black holes*, arXiv:1704.00053 [INSPIRE].

JHEP06(2017)079